Viscoelastic Properties of Polypropylene/Organo-Clay Nano-Composites Prepared Using Miniature Lab Mixing Extruder from Masterbatch

Mohammad Al-haj Ali,[1] Rabeh H. Elleithy[2]

[1]*Chemical Engineering Department, King Saud University (KSU), Riyadh, Saudi Arabia*
[2]*Chemical Engineering Department, SABIC Polymer Research Center, King Saud University (KSU), Riyadh, Saudi Arabia*

Received 9 June 2010; accepted 10 October 2010
DOI 10.1002/app.33573
Published online 15 February 2011 in Wiley Online Library (wileyonlinelibrary.com).

ABSTRACT: Polypropylene (PP) was melt blended with nano organo-clay masterbatch at different ratios; namely 5, 10, and 15 wt % of nano-clay. The effect of organo-clay content on the viscoelastic properties of the nano-composite was studied. A miniature laboratory mixing extruder, LME, was used to blend the nano organo-clay masterbatch with PP at 260°C and 250 rpm. The blend was pelletized first, and then a thin ribbon was extruded. Two viscoelastic tests were performed; frequency sweep at constant temperature of 80°C, and temperature sweep at constant frequency of 1.0 rad/s. As the loading of nano-clay increased, the storage modulus, *G'*, and the thermal resistance increased as well. Different viscoelastic models were tried and 3-elements Maxwell model was found to describe well the viscoelastic properties of the nano-composites. The ratio of the complex modulus to the corresponding matrix modulus at different frequencies was found to vary proportional to the nanoclay loading. This dependency was described reasonably well by modified Guth model using particle aspect ratio of 12.1. © 2011 Wiley Periodicals, Inc. J Appl Polym Sci 121: 27–36, 2011

Key words: blending; clay; thermal properties; nanocomposites; viscoelastic properties

INTRODUCTION

Polypropylene, PP, is a commodity polymer that has various applications ranging from the automotive industry to consumer goods. One way to improve the properties of PP is via controlling its molecular structure, e.g., molecular weight, molecular weight distribution, or stereoregularity of the polymer chain. Another way of changing PP properties is to add additives to PP matrix. These additives could be added, for example, to improve PP low impact resistance, or to increase its use temperature. Inorganic fillers, e.g., calcium carbonate and clay, would fall into the latter category. However, one drawback of adding these fillers is their tendency to decrease other mechanical properties of PP, e.g., ductility. One way to overcome this drawback is to use nanofillers to produce PP nanocomposites.

Nanoclays, which is nano-layered silicates, are widely investigated in the literature because of their abundance and being "green" additive.[1] Additionally, basic understanding of their dispersion and interaction with polymers and, hence, their effect on properties is readily available in the literature.[1,2] Nanofillers, e.g., nanoclays, have the advantage of having nanoscale dimensions which allow the use of a small amount of those fillers to yield improved properties.[1] However, nanofillers tend to be more expensive than traditional fillers and they should be well distributed and dispersed to obtain the desired properties.[2,3] Using masterbatch of nanofillers, i.e., pellets of polymer containing high concentration of nanofillers, could improve the distribution issues associated with polymer nanocomposites. Additionally, the use of masterbatch has an additional health advantage by avoiding the direct use of airborne nanoparticles that could represent a health hazard if not dealt with cautiously. Hence, using masterbatch to produce polymer nanocomposites has gained ground because of its safety, simplicity, and economical advantages. Despite these advantages, to the best of our knowledge there is a limited number of literature that discussed using masterbatch to produce polymer nanocomposites.[4,5]

There are different methods of incorporating nanoclays into the polymer matrix. However, the most industrially accepted one for incorporation noanoclay masterbatch into polymer matrices is via melt blending.[6,7]

The change in mechanical and viscoelastic properties of polymer nano-composites compared with

Correspondence to: R. H. Elleithy (rhelleithy@yahoo.com).
Contract grant sponsor: College of Engineering Research Center, KSU; contract grant number: 21/431.

© 2011 Wiley Periodicals, Inc.

pure polymers is usually evaluated using different models. Two of the most widely used models are Guth model[8] and Haplin-Tsai's equation,[9] eqs. (1) and (2), respectively.

$$G_c = G_0(1 + 2.5\,V + 14.1\,V^2) \quad (1)$$

$$\frac{G_c}{G_0} = \frac{1 + \xi YV}{1 - YV} \quad (2)$$

where V is the volume fraction of the filler, G_c and G_0 are the moduli of the composite and matrix respectively. ξ is a shape parameter dependent upon filler geometry, Y is defined as follows:

$$Y = \frac{(G_c/G_0) - 1}{(G_c/G_0) + \zeta} \quad (3)$$

Note that the original Guth model, eq. (1), is only applicable for spherical fillers. A modified formulation accounts for nonspherical fillers, which are similar to rod-like filler particles, was developed later by Guth[10]:

$$G_c = G_0(1 + 0.67f\,V + 1.62f^2\,V^2) \quad (4)$$

with f is the aspect ratio (length/breadth) of the particles.

In their study of EVA-based nanocomposites, Alexander et al.[11,12] attributed the nonlinear increase in the relative tensile modulus to the decrease of the mean aspect ratio (f) of the primary particles with increasing filler content. To support this explanation, the authors showed that the experimental data follow modified Guth model, eq. (4), with high aspect ratio, $f = 20$, at low filler volume fractions; however, at high filler volume fractions, the modulus follows the model with $f = 12.5$. For carbon-black-filled ethylene-octane elastomers, Flandin et al.[13] found that Guth model, eq. (1), underestimates the shift factor when filler content exceeds 5%(v/v). The model predicts the experimental data well up to filler content of 25% (v/v) when eq. (4) is used with $f = 4.83$.

Wang et al.[14] used the modified Guth theory to estimate the aspect ratio of the fringed-micelle-like crystals of a metallocene-based polyethylene. On the basis of the measured elastic modulus of the polymer, the authors reported that the aspect ratio has an approximate value of 30. The modified Guth model was also used by Frogley et al.[15] to predict the variation of the initial modulus of silicone-based elastomers that have been mixed with single-wall carbon nanotubes (SWNTs) or carbon nanofibers. They found that model predictions agree reasonably with the experimental data using $f = 120$ for SWNTs and $f = 70$ for the carbon nanofibers. Xie et al.[16] reported that the Guth model underestimates the experimental stiffness and yield strength for Poly (vinyl chloride) (PVC)/calcium carbonate ($CaCO_3$) nanocomposites.

Halpin-Tsai model has been applied to estimate the thermal-mechanical properties[17–19] Young's modulus,[20] and reinforcement efficiency[17,21] of polymer nanocomposites as well as the dependence of materials modulus on the individual factor of fillers as aspect ratio and shape.[22]

The main objectives of this work are three folds. First, study the morphology of PP nanocomposite prepared by melt-blend in a miniature lab mixing extruder (LME) using a masterbatch of organo-nano-clay. Second, describe the viscoelastic properties of these PP nanocomposites. Third, assess the validity of using mechanical models, i.e., Maxwell model and Voigt model, to describe the viscoelastic properties of the resulted polymer nanocomposite, and examine the modulus improvement using the modified Guth model.

MATERIAL AND EXPERIMENTAL

An injection molding grade homopolymer Polypropylene, PP78, was purchased from local manufacturer in Saudi Arabia and used in this research. The datasheet indicated that the melt flow index, MFI, of PP78 was 25 g/10 min (DSTM 1238), the Vicat softening temperature was 153°C (DSTM 1525B), and the hardness was 104R (DSTM 785). Commercial PP nano-clay masterbatch with 50 wt % concentration of nano-clay (product name; NanoMax, from Nanocor, USA) was used for the preparation of the nanocomposites. According to the manufacturer, the nano-clay is organophillic montmorillonite (MMT) which has been modified with dimethyl-dihydrogenated tallow ammonium. Henceforth, the used nano-clay is organo- nano-clay. The manufacturer indicated that the neat nano-clay has a fundamental lateral particle size of 300 nm.

The nano-composites were prepared by melt blending the organo-nano-clay masterbatch pellets with PP78 using Laboratory Mixing Extruder (LME), made by Dynisco, USA. LME is a miniature continuous mixing apparatus that has a barrel diameter of about 19 mm and a rotor diameter of about 18.8 mm. LME has a wedge-like helical groove in the barrel and a smooth rotating shaft as shown in Figure 1. This wedge-like helical groove has a length of about 19 mm, a width of 4 mm, and an initial height of 19 mm. This initial height decreased along the length of the helical groove and reached its minimal height by the end of the groove, hence giving the groove a wedge-like shape. The pellets were added from the hopper and manual pressure was continuously applied onto the pellets to aid the mixing process. The blending conditions were: barrel

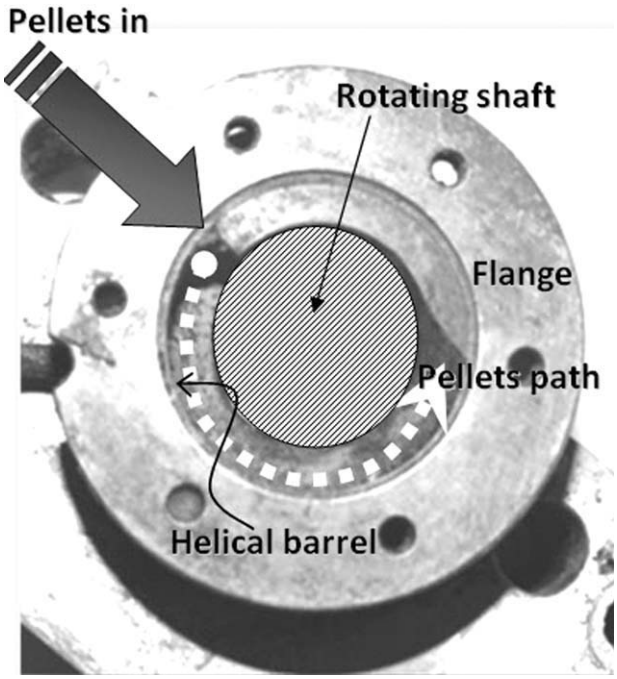

Figure 1 Helical barell of the miniature lab mixing extruder (LME).

temperature = 260°C, die temperature = 265°C, and rotor speed = 250 rpm. Three loadings of the masterbatch were used; 10, 20, and 30%. These loadings yield 5, 10, 15 wt % organo-clay in the nanocomposites. The nanocomposite specimen obtained using PP78 and 5 wt % nano-clay will be called PP78-5. The same nomenclature was used to name the rest of the samples. First, the masterbatch and PP78 pellets were mixed together and then the mix was melt blended and pelletized. Second, these pellets were extruded into ribbons. The width of the ribbons was 7.5 ± 1.5 mm, and their thickness was 0.30 ± 0.05 mm. These ribbons were used for the viscoelastic analysis.

The pellets and ribbons of the nanocomposites were analyzed. The morphology of the nanocomposites was studied via scanning electron microscopy (SEM), JEOL JSM-6360A Japan. The extrudates were first cryogenically fractured to minimize the matrix deformation during fracture. Secondly, the fractured samples were coated with a thin layer of gold, and then the morphology of the fractured surface was examined by the SEM at 15 kV.

Some thermal properties of the nano-composites were evaluated using a differential scanning calorimetry DSC-60 from Shimadzu, Japan. A 7 to 10 mg sample was carefully cut from the pellet to avoid inducing unwanted history to the samples. These samples were analyzed via DSC using the following program. All samples were first heated, then isothermally stabilized at a constant temperature, then cooled, and finally heated up to degradation in air at atmospheric pressure. For the first heating scan, the samples were heated with a constant heating rate of 10°C/min from ambient temperature up to 200°C, then, they were held for 10 min at 200°C to erase their thermal history. Afterward, samples were cooled down to 40°C with a cooling rate of 10°C/min to study the crystallization process. Finally, the samples were heated again for the second time (second heating scan) at a rate of 10°C/min up to 350°C, and the corresponding thermogram was recorded. The melting temperature, T_m was taken as the maximum temperature of the second heating scan endotherm peak. The heat of fusion ΔH was calculated from the second heating scan as well.

The viscoelastic analysis was performed using AR-G2 instrument made by TA Instruments, USA. The analysis was carried under torsion mode on the extruded ribbons using frequency sweep and temperature sweep programs. For both tests, the strain was held constant at 1% which was in the linear viscoelasticity region of PP78 and the nano-composites. The frequency sweep test covered angular frequencies from 0.1 to 100 rad/s, and the test was performed at 80°C. For the temperature sweep test, the temperature range was from 30 to 140°C with 3°C increment, and the frequency was kept constant at 1.0 rad/s.

RESULTS AND DISCUSSION

Morphology

The morphological study showed an even distribution of the nano-particles in the masterbatch [Fig. 2(a)] and the polymeric matrix [Fig. 2(b)] for PP78-15. As mentioned in the experimental section, the organo-nano-clay masterbatch and the polymer were pelletized first, and then the pellets were extruded into ribbons. These double shearing processes combined with the induced shear stress and strain during processing lead to good macro-distribution of the nano-particles as depicted in Figure 2. This figure represents a series of different micrographs at various regions of the nano-composites, all of which indicated a good macro-distribution of the nano-clay within the matrix. Although we used here a miniature lab mixing extruder, the nano clay macro-distribution was acceptable as seen in Figure 2. The area-distribution of particles that have areas of about 1 μm^2 or more was calculated from SEM micrographs using image analysis software, Sigmaplot, USA. Different authors used similar image analysis methodology to study the blending efficiency of polymers and their naocomposites.[23–25] The area distribution for PP78-15 is shown in Figure 3. This result indicated that the majority of the

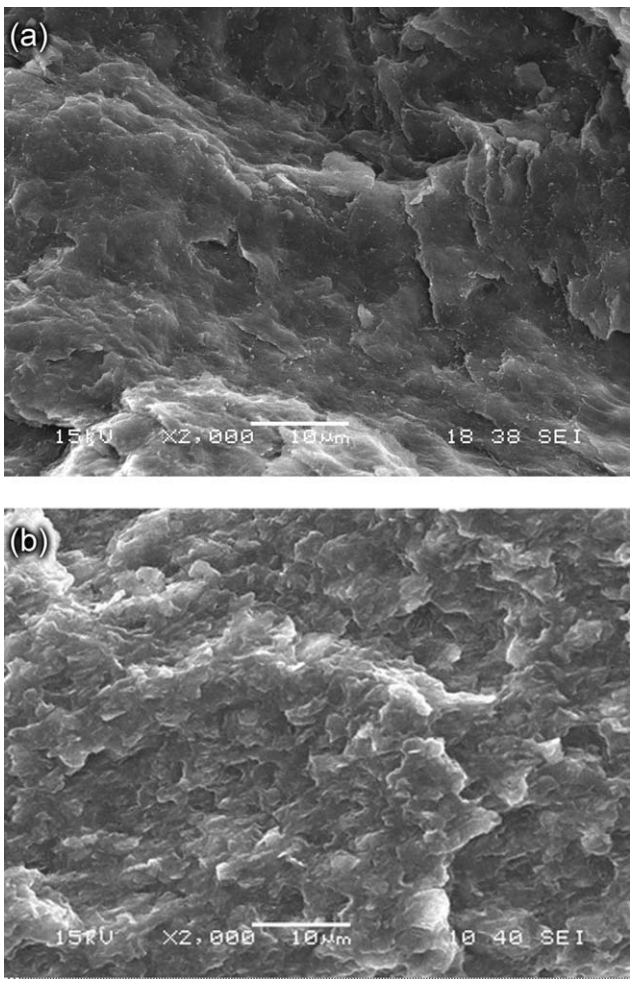

Figure 2 SEM micrographs showing the morphology of [a] nanoclay masterbatch, and [b] PP78-15% nono clay composite.

analyzed particles have area of 1 μm^2 or less. However, note that the total area of the particles analyzed here was less than 2% of the area of the analyzed image. This implied that about 13% of the particles were too small to be analyzed using SEM at this magnification. Therefore, we assumed that a good portion of the particles were indeed in the nano-scale. However, a more detailed analysis is needed to assess the dispersion level of the nano clay into the polymer matrix. That is to say that SEM was successful in assessing the good distribution of the nano clay, but it is not suitable for providing information about the exfoliation of the nano clay particles.

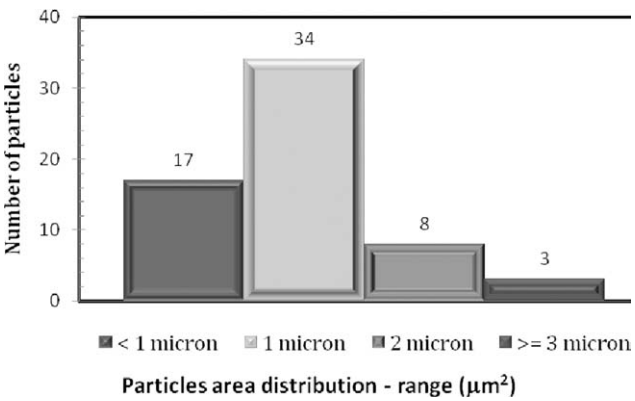

Figure 3 Image analysis PP78-15% indicating the area distribution for particles that have areas of about 1 μm^2 and more.

TABLE I
Thermal Properties of the Nano Composites Tested Here

	Heating		Cooling		
	T_m,°C	ΔH, J/g	T_{oc},°C	T_{c1},°C	T_{c2},°C
PP78-0%	167	102	115	111	–
PP78-5%	165	136	126	113	123
PP78-10%	166	119	129	113	125
PP78-15%	167	115	128	114	124

Thermal analysis

The thermal properties of the nano composites under investigation were calculated from the DSC analysis. The melting temperature, T_m, the heat of fusion, ΔH, the onset of crystallization, T_{co}, and the crystallization temperatures, T_c, are shown in Table I. The addition of nano clay initially reduced T_m due to the initial disturbance of the primary crystallinity[26] and the induction of irregular secondary crystallinity as a result of the presence of the nano clay. However, as the percentage of nano-clay increased further, T_m increased again due to the development of regular secondary crystallinity. This is to say that nano clay acted as heterogeneous nucleating agent. Similar effect of nanoadditives on the thermal properties of polymers was reported by different authors.[27–29] The presence of nano clay initially increased of PP78-5 as indicated in Table I which implies an increase in the crystallinity. As the percentage nano clay increased to 10 and 15%, ΔH decreased which meant that the crystallinity decreased. However, the crystallinity of the nano composites was still higher than that of the neat PP78. Furthermore, the addition of nano clay induced a secondary crystallization temperature as seen from the thermograms in Figure 4. This is to say that the nanocomposites had two crystallization temperatures. First, the T_{c1} which was in the range of the crystallization temperature of neat PP78, therefore it was attributed to the homogeneous crystallization of PP. Second, T_{C2} which was in the range of the crystallization temperature of the nano-clay masterbatch, therefore that was attributed to the heterogeneous nucleation induced by the organo-

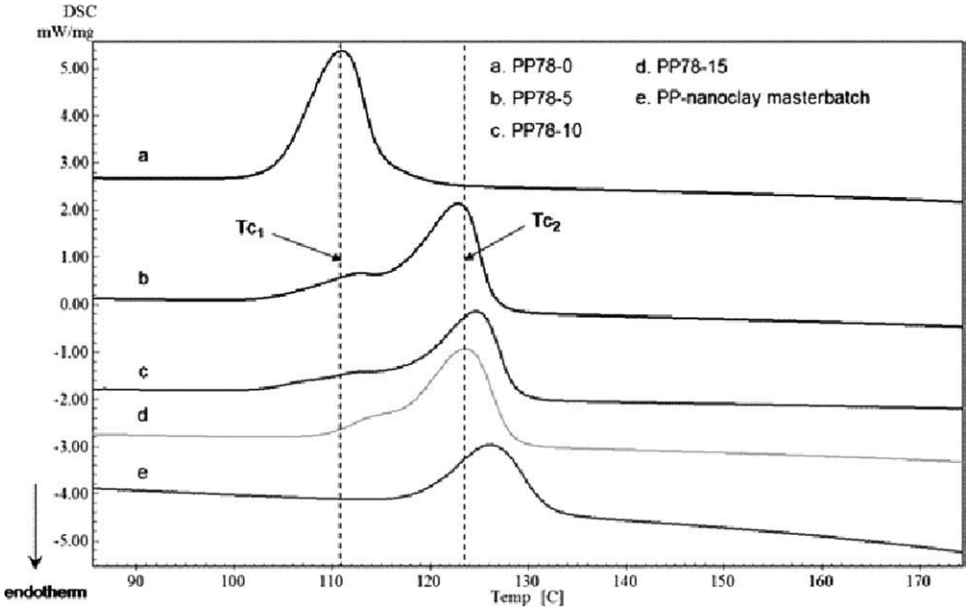

Figure 4 DSC thermograms of nonisothermal crystallization for the PP78-nanoclay composites at a cooling rate of 10°C/min. The curves have been shifted in the y-direction to make them distinguishable.

nanoclay. The resultant was an increase of the crystallization temperatures of the nanocomposites as compared to the neat PP78 resin. This means that the nanocomposites will start and finish crystallization earlier than the neat resin. This will lead to a shorter crystallization time, which is of a great economical implication as it allows a shorter cooling cycle during manufacturing.

Viscoelastic analysis: Experimental

The effect of temperature on the storage modulus (G') of the tested material is shown in Figure 5. For all temperatures, the nanocomposites had higher G' than the neat resin, and PP78 + 15 had the highest G' of all. Several authors reported similar increase in the modulus as the percentage of the nanoclay increased.[30–33] Nanoclay tends to accumulate in the amorphous region of the matrix similar to interstitial defects seen in alloying. Figure 6 schematically illustrates this concept. For neat resin, Figure 6(a), the free volume could be visualized as the voids within the amorphous region. As the nanoclay is added to the resin, the majority of the clay will go to the amorphous region rather than the crystalline region. Depending on the relative size of the nanoclay to the size of the amorphous voids, two situations could arise. First, if the nanoclay is relatively smaller than the amorphous voids, it will go there with minimal disturbance to the chain conformations, Figure 6(b). This could lead to a decrease of the free

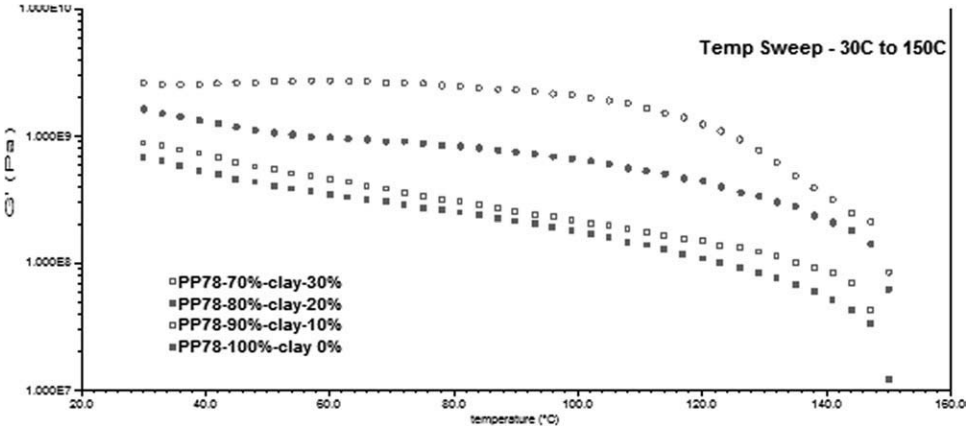

Figure 5 Temperature sweep at 1 rad/s of PP78 nano composites depicting the relation between G' and temperature.

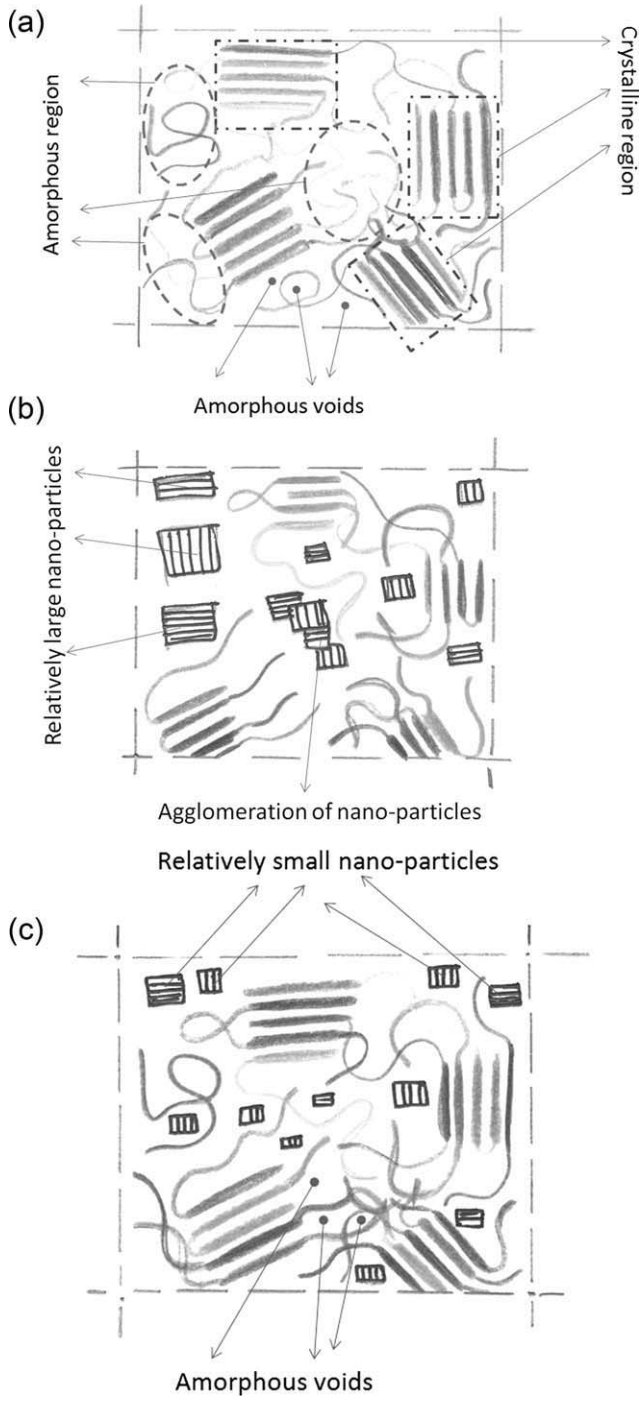

Figure 6 Schematic illustation of neat resin (a), nanocomposite with relative large nanoparticles (b) and nanocomposite with relatively small nanoparticles (c).

volume of the matrix.[34] Second, if the nanoclay is relatively larger than the amorphous voids, the presence of the nanoclay in the amorphous region would disturb the chain conformations as presented in Figure 6(c). This could lead to an increase of the free volume of the matrix.[35] In the same system, we can observe both the increase and decrease depending on the nonmaterial loading.[36] The decrease of the free volume will reduce the available space for molecules to move in, which in turn will limit the molecular mobility of the PP chains.[37] Moreover, nanoclay particles acted as obstacles which hindered the molecular mobility of the nanocomposites as compared to the neat resin. This interaction between the nano clay and the matrix depends on the interfacial area shared between the PP and the nano clay. As the interfacial area increased, the interaction increased, and hence the chains were more restricted. Additionally, the increased crystallinity of the nanocomposites restricted the molecular mobility even further. These three factors; free volume changes, nanoclay-PP interaction, and increased crystallinity; and the interaction between the three factors led to the increase of the nanocomposits' modulus as compared with the neat resin. This explained the increase of the storage modulus of the nano composite by increasing the level of the nano clay loadings or the level of the interaction between PP and nano clay.[38] In addition to increasing the modulus, adding nano clay stabilized the modulus of the nanocomposites with temperature when compared to the neat resin as seen in Figure 5. This effect was not very pronounced at 5% nano clay but was obvious at 15%. The behavior of the nanocomposites at different temperatures, Figure 5, could be grouped into two sets, [A] PP78, PP78 + 5, and [B] PP78 + 10, PP78 + 15. For set [A] the decrease of G' with temperature is more steep than that of set [B]. The slow decrease of G' with temperature is used as an indication of material resistance to the increase of temperature. From this token, PP78 + 15 showed the longest stability of G' with temperature, and hence is considered the most thermally stable. The modulus of PP78 + 15 was stable at about 2.5 GPa over a temperature range from 30 to 90°C. This wide range of constant modulus increased considerably the usage temperature of PP78 + 15 which is a definite benefit of using nano clay. This phenomenon was attributed to the restriction of the molecular mobility as discussed earlier.

The relationship between the storage modulus (G') and the angular frequency (ω) at 80°C is depicted in Figure 7. As the frequency increased the modulus of the PP78 and its nano-composites increased as well due to the increased difficulty of the molecular mobility at higher frequencies. Similar results were seen by different authors.[30,32-33,39] Moreover, this figure shows that G' increased proportionally to the loading of the nano clay. This same observation was reported by other authors.[32,33,39] The modulus of PP78 and PP78 + 5 was close to each other, and then there was an abrupt increase in the modulus for PP78 + 10 and PP78 + 15. One possible

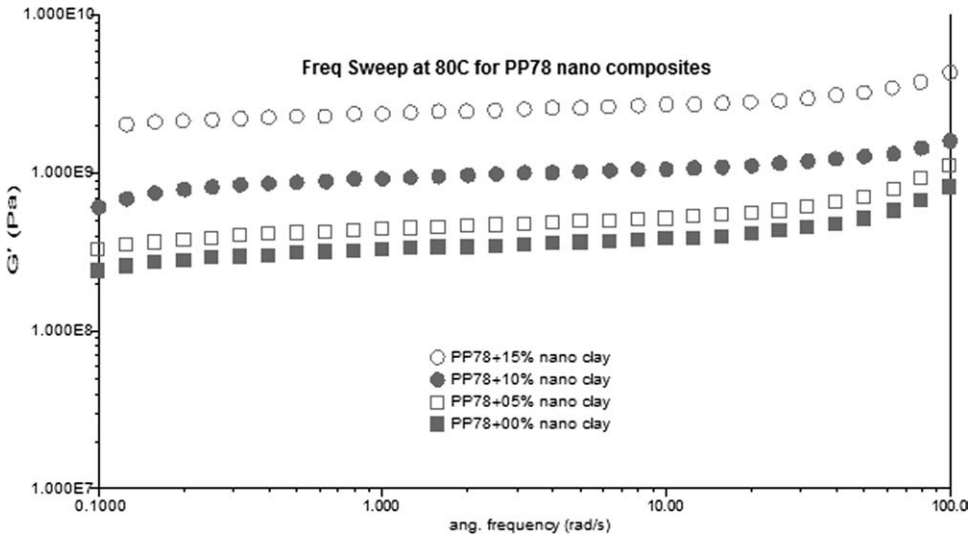

Figure 7 Frequency sweep at 80°C of PP78 nano composites depicting the relation between G' and ω.

TABLE II
Transition Modulus and Frequency for the Tested Materials

	Transition [1] to [2]	
	G', MPa	ω, rad/s
PP78	410	18
PP78-5	630	21
PP78-10	1200	44
PP78-15	3000	55

explanation of this abrupt increase could be the increased interfacial area between PP78 polymer matrix and nano-clay which resulted in more interaction between the PP and the nano-clay. This further restricted the polymer mobility and hence increased its modulus. For all tested materials, the relation between G' and ω could be divided into two regions[1]; low-medium frequency and[2] high frequency. In the first region, G' increased moderately with ω. Whereas, in the second region G' increased sharply with ω. The transition between these two regions moved to a higher frequency, or shorter time, as the loading of the nano clay increased which is an indication of the restricted mobility of the polymer molecules as the nano clay loading increased. The G' and ω values of these transitions are listed in Table II. It was also found that the transition frequency is linearly proportional to the loading of nano clay as shown in Figure 8.

Viscoelastic analysis: Modeling

The variation of complex modulus with nanoclay loading at three frequencies was fitted using different correlations; it was found that an exponential function multiplied by a constant gives acceptable predictions as shown in Figure 6; model parameters are summarized in Table IV. Interestingly, the exponent term in this equation can be considered as constant; meanwhile the variation in the leading term

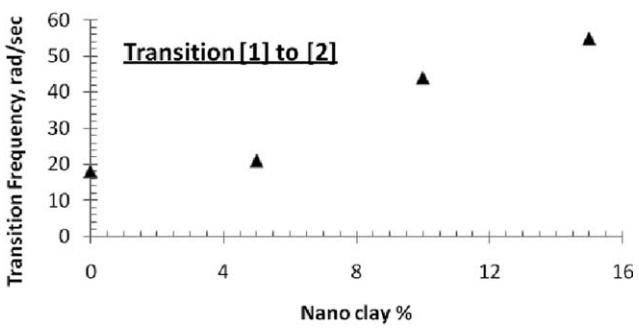

Figure 8 The relation between the transition Frequency and the nano clay loading for PP78 nano composites at 80°C.

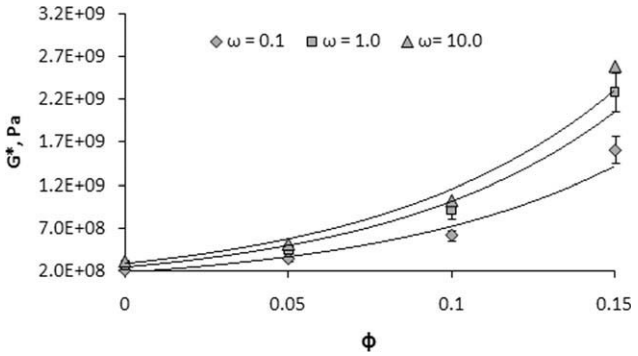

Figure 9 The variation of complex modulus with nanoclay loading at different angular frequencies (in rad/s).

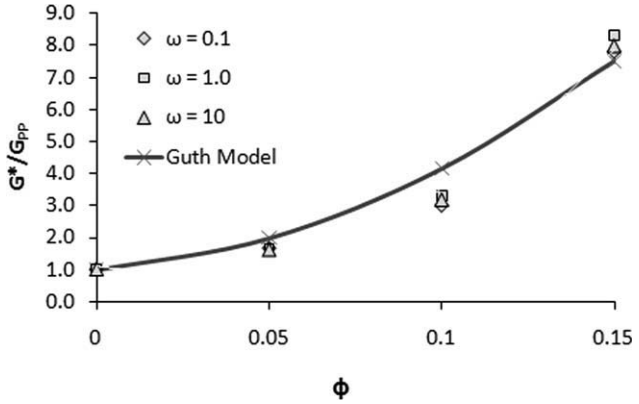

Figure 10 The variation of normalized complex modulus with nanoclay loading at different angular frequencies.

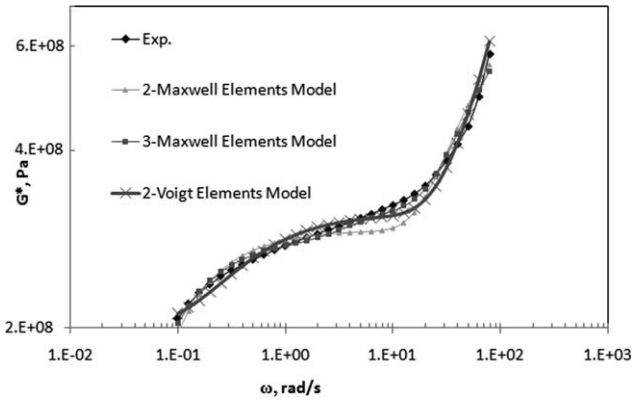

Figure 11 Comparison between the predictions of different viscoelastic models for neat PP.

with frequency can be also modeled using the exponential function, see eq. (5).

$$G^*(\omega, \phi) = A(\omega) \cdot \exp(-0.691 \cdot \phi)$$
$$A(\omega) = 2 \times 10^8 \cdot \exp(-0.208 \cdot \omega) \quad (5)$$

The experimental data in Figure 9 were normalized by dividing G^* of the nanocomposites by the corresponding modulus of neat polypropylene as shown in Figure 10. It can be seen from both figures that G^* of the nanocomposites increase relative to unfilled matrix. This increase depends on nanoclay loading, at 5 wt % clay, a 160% increase in the G^* occurred compared with 320% increase at 10 wt % clay loading. It should be noted that the improvement in moduli reported in this work is comparable with that reported in the literature. Paglicawan et al.[32] studied polystyrene-*b*-poly(ethylene/butylene)-b-polystyrene (SEBS) triblock coplymer with the presence of multi-wall carbon nanotubes (MWNTs). They reported around 200% increase in storage modulus at 5 wt % MWNT loading compared to 1 wt % loading. Prashantha et al.[33] found that the flexural modulus increased by a factor of 1.5 when the concentration of MWNTs is 2 wt %. In these two investigations, effective dispersion of nanotubes was reported.[31](2007) concentrated on high density polyethylene (HDPE)-MMT nanocomposites. For 8 wt % nanocomposite, the authors reported 68% increase in the Young's modulus though there was no sign of exfoliation. Austinand and Kontopoulou[30] created a hybrid nanocomposite structure by compounding organoclay into blends of maleated polyolefin elastomers with PP. At $\omega = 0.1$ rad/s, the authors reported large increase in G', compared to unfilled matrix, that varies between one order of magnitude to three order of magnitudes for 2 wt % and 20 wt % nanoclay loadings, respectively. This difference is considerably reduced to one order of magnitude when ω is increased to 100 rad/s.

Figure 10 reveals that these moduli can be represented by a master curve which can be considered as a description for the polymer-nanocomposite material. Also, It can be seen from this figure that the modified Guth equation agrees reasonably with the experimental data using $f = 12.1$. This value agrees with what was reported earlier by Alexander et al.[11,12]

Three mechanical models were used to fit complex viscosity (G^*) versus angular frequency experimental data. Fitting results are shown in Figures 10 and 11 and summarized in Tables III and IV.

Figure 11 shows a comparison between the fitted models and the experimental data for neat polypropylene samples. The prediction obtained by the 2-Maxwell elements model is the worst with relatively large prediction errors that reach about 10%. The predictions of three Maxwell-elements model

TABLE III
Fitting Parameters for 3-Elements Maxwell Model Using Different Nano Clay Loadings

ϕ, %	G_1, Pa	G_2, Pa	G_3, Pa	τ_1, s	τ_2, s	τ_3, s	R^2
0	2.84E+08	5.00E+07	4.70E+08	30.00	0.22	0.0160	0.984
5	4.55E+08	7.75E+07	4.60E+08	34.50	0.40	0.0163	0.989
10	9.32E+08	9.90E+07	5.38E+08	25.88	0.51	0.0195	0.994
15	2.38E+09	2.28E+08	8.34E+08	25.88	0.51	0.0195	0.990

TABLE IV
Fitting Parameters for the Exponential Function

ω, rad/s	A, Pa	Exponent	R^2
10	1.45E+08	0.705	0.982
1.0	1.22E+08	0.692	0.980
0.1	9.55E+07	0.675	0.977

are the most accurate with prediction errors that do not exceed 5% for the whole angular frequency range. Two-Voigt elements model predicts experimental data well with maximum error of about 7%.

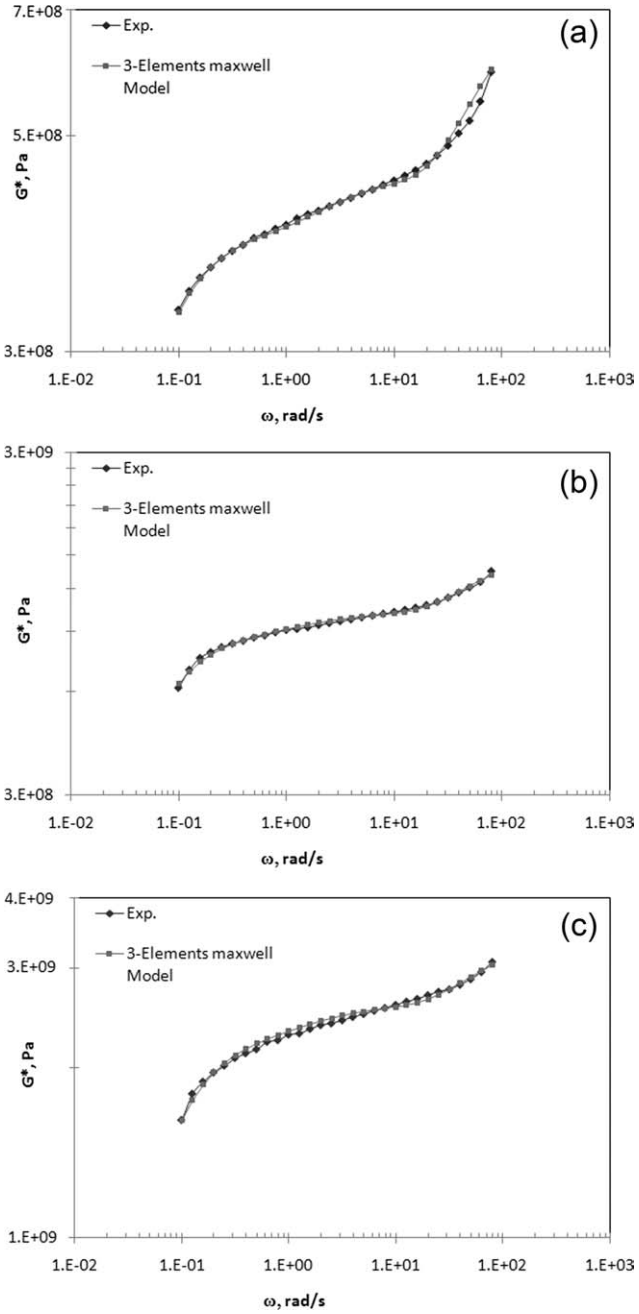

Figure 12 Experimental versus the predictions of 3 Maxwell elements model for 5% (a), 10% (b) and 15% (c) nanoclay loadings.

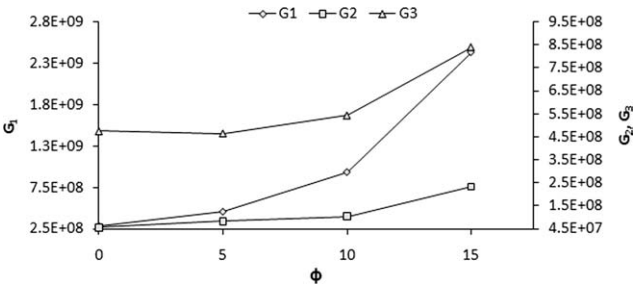

Figure 13 The variation of fitted modulus with nanoclay loading.

The 3-element Maxwell model successfully described the variation of complex modulus with angular frequency for the entire range of nanoclay loadings considered in this work, Figures 12(a–c). Conversely, both 2-elements Voigt and -Maxwell models could not predict the experimental data for all nanocaly loadings. Note that, for 5% nanoclay loading, 3-Voigt elements model predicted the experimental data very well up to angular frequency of around 1.0 rad/s. However, at higher frequencies, the model could not capture the variations in experimental data though it predicted the experimental data of neat polypropylene very well for the entire range of angular frequencies.

Figure 13 shows the variation of the three fitted modulus parameters, namely G_1, G_2, and G_3, with nanoclay loading (ϕ). The change in G_1 with changing nanoclay loading, i.e., $\Delta G_1/\Delta\phi$, is approximately constant for the entire range of ϕ. G_2 varies differently with ϕ; $\Delta G_2/\Delta\phi$ is almost constant for nanoclay loadings less than 10%. However, for higher loadings, $\Delta G_2/\Delta\phi$ became about six times higher. G_3 decreased for nanoclay loadings below 5%, and then it increased with increasing the loading.

CONCLUSIONS

PP-organo clay nanocomposites containing 5, 10, and 15 wt % of organoclay was prepared using nanoclay masterbatch. The preparation took place via two steps of melting blend using miniature laboratory mixing extruder. The nanoclays were distributed well in the PP matrix as shown by SEM. The incorporation of the well-distributed nanoclay lead to significant improvements in the thermal and viscoelastic properties of PP. Some of these improvements are the increase in the crystallization temperature, the crystallinity, the modulus, and the temperature stability.

It was found that the viscoelastic properties of the nanocomposite can be accurately described using a group of three Maxwell elements in parallel. The use of three Voigt elements in a series arrangement was

proved to be suitable up to nanoclay loadings of 5 wt % and angular frequency of 1.0 rad/s. The division of the complex modulus of the nanocomposite by the corresponding matrix complex modulus gave a "master curve" that was dependent only on the nanoclay loading. This master curve can be described well using the modified Guth model with mean aspect ratio of particles that equaled 12.1.

The authors are grateful to SABIC Polymer Research Center at KSU for allowing us to use their equipment. They appreciate the effort that Achmad Chafidz put in generating some of the data used in this work. They are also thankful to Dr. Ilias Ali for his fruitful suggestions and contribution to this work.

References

1. Alexandreand, M.; Dubois, P. J Mater Sci Eng 2001, 28, 1.
2. Lei, S. G.; Hoa, S. V.; Ton.-That, M-T. J Compos Sci Technol 2006, 66, 1274.
3. Giannelis, E. P. Appl Organometallic Chem 1998, 12, 675.
4. Lee, S. H.; Kim, M. W.; Kimand, S. H.; Youn, J. R. Eur Polym J 2008, 44, 1620.
5. Prashantha, K.; Soulestin, J.; Lacrampe, M. F.; Krawczak, P.; Dupin, G.; Claes, M. Compos Sci Technol 2009, 69, 1756.
6. Modesti, M.; Lorenzetti, A.; Bon, D.; Besco, S. Polymer 2005, 46, 10237.
7. Pavlidou, S.; Papaspyrides, C. D. Prog Polym Sci 2008, 33, 1119.
8. Guth, E.; Gold, O. Phys Rev 1938, 53, 322.
9. Halpin, J. C.; Kardos, J. L. Polym Eng Sci 1976, 16, 344.
10. Guth, E. J Appl Phys 1945, 16, 20.
11. Alexander, M.; Beyer, G.; Henrist, C.; Cloots, R.; Rulmont, A.; Jerome, R.; Dubois, P. Chem Mater 2001, 13, 3830.
12. Alexander, M.; Beyer, G.; Henrist, C.; Cloots, R.; Rulmont, A.; Jerome, R.; Dubois, P. Macromol Rapid Commun 2001, 22, 643.
13. Flandin, L.; Hiltner, A.; Baer, E. Polymer 2001, 42, 827.
14. Wang, C.; Chu, M.-C.; Lin, T.-L.; Lai, S.-M.; Shin, H.-H.; Yang, J.-C. Polymer 2001, 42, 1733.
15. Frogley, M. D.; Ravich, D.; Wagner, H. D. Compos Sci Technol 2003, 63, 1647.
16. Xie, X. L.; Liu, Q. X.; Li, R. K. Y.; Zhou, X. P.; Zhang, Q. X.; Yu, Z. Z.; Mai, Y. W. Polymer 2004, 45, 6665.
17. Brune, D. A.; Bicerano, J. Polymer 2002, 43, 369.
18. Yoon, P. J.; Fornes, T. D.; Paul, D. R. Polymer 2002, 43, 6727.
19. Goyal, R. K.; Tiwari, A. N.; Negi, Y. S. Mater Sci Technol 2008, 491, 230.
20. Zheng, X. Y.; Forest, M. G.; Lipton, R.; Zhou, R. H. Continuum Mech Therm 2007, 18, 377.
21. Fuchs, C.; Bahattacharyya, D.; Friedrich, K.; Fakirov, S. Compos Interfaces 2006, 13, 331.
22. Fornes, T. D.; Paul, D. R. Polymer 2003, 44, 4993.
23. Carastan, D. J.; Vermogen, A.; Masenelli-Varlot, K.; Demarquette, N. R. Polym Eng Sci 2010, 50, 257–267.
24. Jang, B. Z.; Uhlmann, D. R.; Sande, J B. V. Polym Eng Sci 1985, 25, 643.
25. Plochocki, A. P.; Dagli, S. S.; Curry, J. E.; Starita, J. Polym Eng Sci 1989, 29, 617.
26. Al-haj Ali M.; Elleithy, R.; Al-Zahrani, S. M.; Chafidz, A. p. 246, ANTEC 2010, Orlando, USA.
27. Ge, C.; Shi, L.; Yang, H.; Tang, S. Polym Compos 2010, 31, 1504–1514.
28. Ren, J.; Yu, T.; Li, H.; Ren, T.; Yang, S. Polym Compos 2008, 29, 1145–1151.
29. Zha, L.; Fang, Z. Polym Compos 2010, 31, 1258–1264.
30. Austin, J. R.; Kontopoulou, M. Polym Eng Sci 2006, 46, 1491.
31. Chu, D.; Nguyen, Q.; Baird, D. G. Polym Compos 2007, 28, 499.
32. Paglicawan, M. A.; Kim, J. K.; Bang, D. S. Polym Compos 2010, 31, 210.
33. Prashantha, K.; Soulestin, J.; Lacrampe, M. F.; Krawczak, P.; Dupin, G.; Claes, M. Compos Sci Technol 2009, 69, 1756.
34. Brik, M. E.; Titman, J. J.; Bayle, J. P.; Judeinstein, P. Journal of Polymer Science. Part B: Polym Phys 1996, 34, 2533.
35. Koo, J. Polymer Nanocomposites: Processing, Characterization, and Applications; Mc-Graw Hill: New York, 2006.
36. Utracki, L. A. Polym Degrad Stabil 2010, 95, 411.
37. Ferry, J. Viscoelastic Properties of Polymers; John Wiley & Sons, Inc.: New York, USA, 1980.
38. Kontou, E.; Niaounakis, M. Polymer 2006, 47, 1267.
39. Yazdani, H.; Morshedian, J.; Khonakdar, H. A. Polym Compos 2006, 27, 491.